

Design of Mechanically Robust High- T_g Polymers: Physical Properties of Glassy Poly(ester carbonate)s with Cyclohexylene Rings in the Backbone

Xiangyang Li^{†,§} and Albert F. Yee^{*,‡}

Macromolecular Science and Engineering, University of Michigan, Ann Arbor, Michigan 48109, and Materials Science and Engineering, Macromolecular Science and Engineering, University of Michigan, Ann Arbor, Michigan 48109

Received April 29, 2003; Revised Manuscript Received October 8, 2003

ABSTRACT: The incorporation of *trans*-cyclohexylene (C-ring) groups into the main chains of glassy polymers increases polymer chain dynamics. With the increase in *trans*-C-ring content in the main chain, both the coefficient of thermal expansion (CTE) of bulk specimens and the CTE of nanosized holes in these glasses increase. *Trans*-C-ring incorporation also increases T_g and improves chain packing. These multiple effects are proposed to be due to ring inversion and the shape of the *trans*-C-rings: The ring inversion introduces enhanced local chain motion, which is proposed to reduce interchain interaction by decreasing the contact area and contact frequency between polymer chains. The *trans* configuration of C-rings has the effect of extending the polymer chains, which results in increased persistence length and improved chain packing. The increased persistence length leads to increased T_g , even though the decreased interchain interactions would have the opposite effect. Substituting some *trans*-C-rings by *cis*-C-rings results in marked decrease in persistence length and therefore a significant decrease in T_g . This further points to a correlation between persistence length and T_g .

1. Introduction

Main-chain segmental molecular motions in polymer glasses are thought to play a crucial role in their mechanical properties, such as yield stress, craze stress, and impact strength;^{1–4} furthermore, it was proposed that these molecular motions can be enhanced by some types of conformational transitions in the main chain, such as the ring inversion of cyclohexylene group (C-ring).^{2–5} In a companion paper,⁶ the synthesis, characterization, and the secondary relaxation behavior of three series of high- T_g glassy polymers with the incorporation of main-chain C-rings are reported. The chemical structures of these polymers are shown in Figure 1, and their T_g s are listed in Table 1. One characteristic of these polymers is that they possess relatively stiff backbone segments. In this paper, the effect of main chain C-ring incorporation on some physical properties, such as the coefficient of thermal expansion (CTE), and the glass transition temperature is reported. The insertion of C-rings is expected to provide extra dynamics to these otherwise stiff chain polymers. The coefficients of thermal expansion of polymers have contributions from both in-chain and interchain components. Since bonds in polymers are very anisotropic, the expansion coefficient along the chain is much smaller than that between the chains. Consequently, the contribution from the intrachain component toward the total thermal expansion coefficient is negligible. This point was well recognized by previous researchers.^{7–12} For polymers, as stated by Stachurski,¹¹ “a 3-dimensional macroscopic volume expansion is always derived from 2-dimensional expansion orthogonal to the chain axis.”

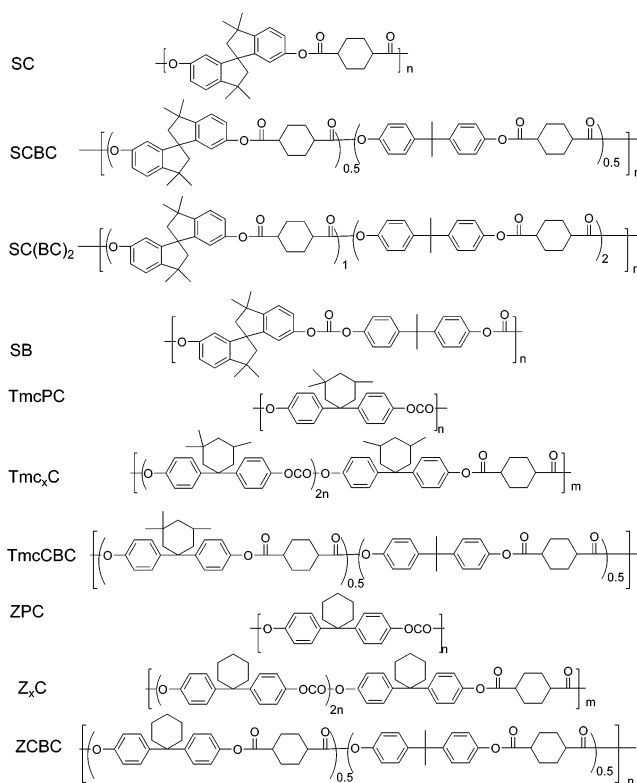


Figure 1. Chemical structures and short names for all the polycarbonates, polyesters, and poly(ester carbonate)s, wherein x represents the average number of repeat units within each bisphenol polycarbonate block.

Since the discovery of polymer glasses, scientists have proposed theories or empirical correlations to describe and understand the dependence of T_g on molecular parameters. It has been generally recognized that intermolecular interaction (as indicated by cohesive energy density CED), intramolecular parameter (such

[†] Macromolecular Science and Engineering.

[‡] Materials Science and Engineering, Macromolecular Science and Engineering.

[§] Current address: Lexan Technology, GE Plastics, Mount Vernon, IN.

* Corresponding author. E-mail afyee@engin.umich.edu.

as chain steric factor σ , characteristic ratio C_∞ , persistence length L_p , and chain geometry play major roles in determining the glass transition temperature.^{13–16} The correlations established so far have been quite successful in describing some classes of polymers, yet none has been successful in fitting polymers containing aromatic groups in their backbones. The reason for this is difficult to pinpoint, but it is possible that one key point is how chain stiffness of these polymers can be described. For polyolefins and other simple polymers with C–O backbones, C_∞ and σ appear to be good molecular parameters for describing their chain stiffness. C_∞ describes chain stiffening effects by rigid bond angles and restricted rotation, while σ only indicates chain stiffening by restricted rotation. These two parameters fail to take into account chain stiffening by internal structures such as rigid cyclic rings, etc.¹⁷ As put by Birshtein,¹⁷ “A natural measure of flexibility is here only the absolute value, namely the length of Kuhn segment..., or the persistent length.” The concept of persistence length L_p was introduced a long time ago by Kratky and Porod¹⁸ as a parameter for their worm-like chain model. This model is widely used for describing conformational characteristics of less flexible chains.^{19,20}

By knowing the effects of main-chain C-ring incorporation on CTE and T_g , their effects on intermolecular forces and chain stiffness can be inferred. To obtain the CTE of nanometer voids, a technique called positron annihilation lifetime spectroscopy (PALS) was used. Extensive research using PALS has been done to examine the effects of thermal history,²¹ pressure,²² and mechanical stress²³ on nanometer voids in polymers. In PALS, the lifetime (τ_3) of orthopositronium (o-Ps) is used to measure the size of nanometer voids,^{24,25} while its relative intensity (I_3) is interpreted to be proportional to the number density of holes.^{26,27}

It should be pointed out that o-Ps cannot probe all hole sizes. Because o-Ps has a lifetime of about 2 ns in polymers, it cannot detect holes generated by fluctuations with frequencies higher than $\sim 10^{10}$ Hz. If the hole size is too small, the o-Ps is also unable to localize in it before annihilation. The minimum void radius is thus around 1.94 Å.²⁸ If the void radius is greater than approximately 20 Å, the lifetime of Ps is insensitive to small changes in size,²⁹ thereby losing its usefulness. Therefore, PALS is capable of detecting molecular voids with radii ranging from 2 to 20 Å. However, by using classical mechanics, the upper limit to voids that can be probed has been extended by 2 orders of magnitude. It should be noted that although there are definite similarities, the nanometer voids measured by PALS are not identical to the “free volume” liberally used in much of the polymer literature. The most obvious difference is that PALS can detect static nanometer voids such as those in nanoporous solids but cannot detect nanometer voids generated by rapid molecular motion above 10^{10} Hz. Presumably, the definition of “free volume” includes volume generated by such fast motions.

The interpretation of the correlation between τ_3 and the hole size is widely agreed upon, but the correlation between I_3 and the number density of holes is being debated. It has been reported that I_3 can be affected by many factors, such as the data fitting artifacts,²⁶ source strength and irradiation time,^{26,30,31} and electrical field.³² Recently, it has been reported that hole volume fraction correlates much better with τ_3 than with I_3 .³³ Because

Table 1. Molecular Weight and Glass Transition Temperature of the Polymers

polymer	M_n	M_w	$T_g/^\circ\text{C}$
SC	51K	778K	275
SCBC	39K	77K	246
SB	126K	262K	198
TmcPC	106K	204K	240
Tmc ₅ C	80K	137K	245
Tmc ₃ C	75K	119K	252
Tmc ₁ C	40K	84K	283
TmcCBC	66K	131K	257
ZPC	32K	79K	182
Z ₅ C	92K	164K	190
Z ₃ C	63K	109K	195
Z ₁ C	52K	111K	228
ZCBC	87K	171K	220

of the controversies involving the interpretation of I_3 , in this work, only information extracted from τ_3 will be discussed.

2. Experimental Section

2.1. Sample Preparation and Testing Conditions for CTE. The polymers studied in this work are given in Table 1 and Figure 1. Their synthesis is described in a companion paper.⁶ Cyclohexylene groups (C-rings) were incorporated in the main chain of polymers made from two rigid and bulky monomers, spirobiindane bisphenol (SBI) and trimethylcyclohexylbisphenol (Tmc), and a less rigid monomer, cyclohexylbisphenol (BPAZ). CTE tests were performed on amorphous films with typical dimensions of 20 mm \times 5 mm \times 0.1 mm (length \times width \times thickness). The films were prepared from dry polymer powders dissolved in dichloromethane, forming 5% solutions. Each solution was filtered through a microfilter and cast on a clean glass slide to form a film. The solvent was evaporated slowly at room temperature overnight. The films were then floated off the glass slides with distilled water. They were placed under vacuum at 65 $^\circ\text{C}$ for 48 h to remove any residual solvent. All the films were visually clear and were confirmed to be amorphous by DSC.

The CTE tests were performed using a TA Instruments DMA model 2980. No further thermal treatment was applied prior to the DMA tests. The controlled force mode was used with a static force of 0.1 N. The samples were run in an isostep mode from -120 to 100 $^\circ\text{C}$ in 10 $^\circ\text{C}$ intervals with cooling achieved by a liquid nitrogen cooling accessory. The samples were held isothermally for 5 min at each temperature, giving around 10 min for thermal equilibration at each temperature. The specimen length at each temperature was recorded by computer for 1 min at a sampling rate of 2 points/s. Each complete run took about 4 h.

2.2. Positron Annihilation Lifetime Spectroscopy. Square specimens of the polycarbonates, polyesters, and poly(ester carbonate)s were cut from films prepared for bulk CTE tests. These square films with dimensions of 10 mm \times 10 mm \times 0.1 mm (length \times width \times thickness) were made into film stacks with total thickness of 1 mm. A 80 μCi $^{22}\text{NaCl}$ positron source was sandwiched between two stacks of films and then wrapped inside a 7 μm tin foil. The sandwich was then enclosed completely in a copper sample holder, which was wrapped inside a heating tape. The entire assembly was placed in a temperature chamber equipped with a temperature controller which kept each selected temperature within ± 1 $^\circ\text{C}$.

The positron lifetime spectra were obtained by a conventional fast-timing coincidence method.²⁹ Signals from the start and stop detectors, consisting of scintillators coupled to photomultipliers (Amperex XP2020 with S563 bases), were processed by two constant fraction differential discriminators (CFDD, Ortec583) with the start energy window normally set for the ^{22}Na 1.28 MeV γ -ray (indicating the birth of a positron) and the stop set for the 0.511 MeV annihilation γ -rays. The time interval between the start and stop signals from the CFDDs was converted to an output pulse whose height is proportional to the time interval by a time-to-amplitude

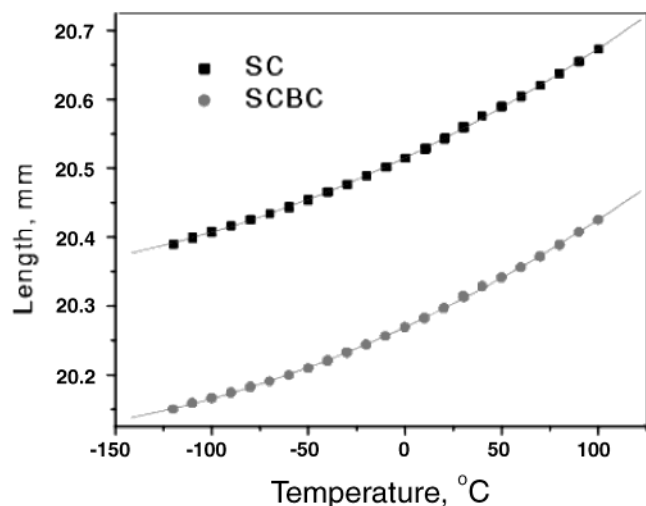


Figure 2. Length change with temperature for SC and SCBC.

converter (TAC, Ortec567). The TAC output pulses were then digitized by an analog-to-digital converter (ADC, ND581) and were recorded by an integrated multichannel analyzer (ND9900) through an ethernet compatible module (AIM, ND556) into a Micro VAX 3100 workstation (Digital) that performed both data acquisition and analysis.

For each specimen, data were collected over a 30 min period at a coincidence rate of approximately 1800 counts/s, resulting in a spectrum with approximately 2 million counts. The PALS measurements were performed in the temperature range of -140 to 200 °C with a temperature increment of either 10 or 20 °C. The lifetime spectra obtained were resolved into three exponential components: the respective lifetimes and relative intensities, together with time resolution, were determined by the computer program PFPOSFIT³⁴ (details given in ref 35). The full width half-maximum of the time resolution prompt curve was 280 ps as determined by a ^{60}Co source. Because positron annihilation in the source material only contributed a small constant fraction (usually a very few percent) to the total annihilation events, and relative changes in lifetimes are the main concerns in the current experiments, source corrections in the fitting procedure were not made. The first (τ_1) and second (τ_2) components, which were associated with p-Ps and bulk positron annihilation events, respectively, were found to be unaffected by the temperature change and will not be considered further. The third components, I_3 and τ_3 , were taken to be due to o-Ps pick-off annihilation. The correlation between τ_3 and hole size is obtained through eq 1.^{24,25}

$$\tau_3^{-1} = \lambda_{\text{spin}} G + \Lambda_{\text{o-Ps}}(1 - G) \quad (1)$$

where $\lambda = 2 \text{ ns}^{-1}$, $G = 1 - R/(R + \Delta R) + (1/2\pi) \sin[2\pi R/(R + \Delta R)]$, R is the radius of the hole, and ΔR is 1.612 Å.²⁹ Further details of the relevant theories and assumptions are given in refs 24, 25, 34, and 35.

3. Results and Discussion

3.1. The Coefficient of Thermal Expansion. The length changes with temperature for the polymers studied in this work are shown in Figures 2–4. A second-order polynomial can fit the data for all the polymers quite well. First-order polynomial equations were in fact used for the determination of the linear thermal expansion coefficients (LCTE). LCTE values at the temperature range of -120 to 100 °C are shown in Figures 5–7. Figure 5 shows that SC and SCBC have very similar thermal expansion coefficients within the temperature range studied. For both the Tmc series and BPAZ series, with the increase in main-chain C-ring content, the LCTE increases. A linear correlation be-

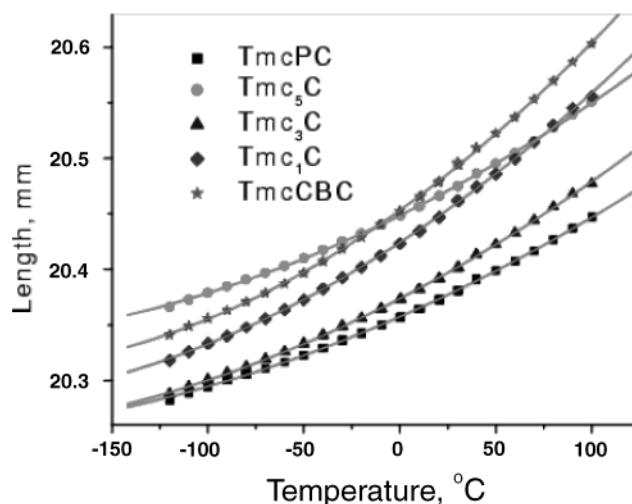


Figure 3. Length change with temperature for polymers of Tmc series.

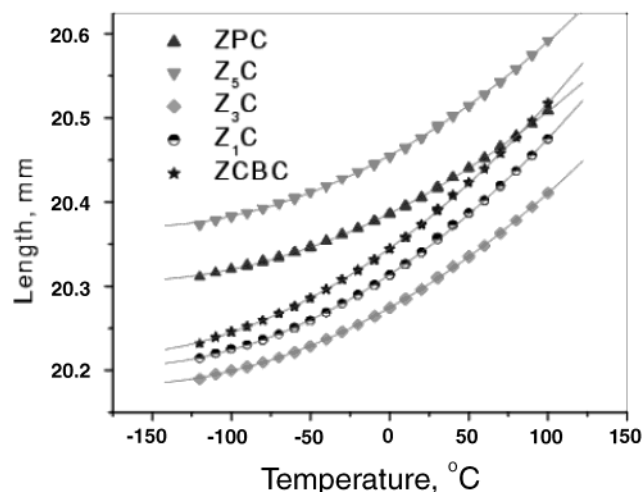


Figure 4. Length change with temperature for polymers of BPAZ series.

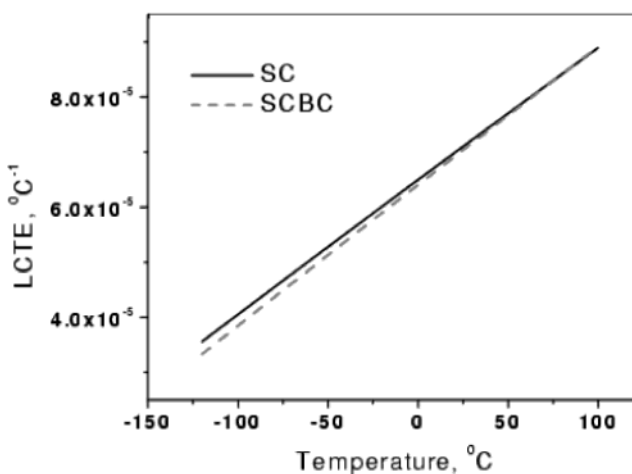


Figure 5. LCTE change with temperature for SC and SCBC.

tween the relaxation strength and the total C-ring concentration is reported in the companion paper.⁶ It is important to see whether such a correlation can be established in terms of LCTE. Shown in Figure 8 is the plot of LCTE of BPAZ polymers at 25 °C vs the total concentration of C-rings. Obviously, the correlation in LCTE value for ZCBC is invalid: ZCBC has the greatest

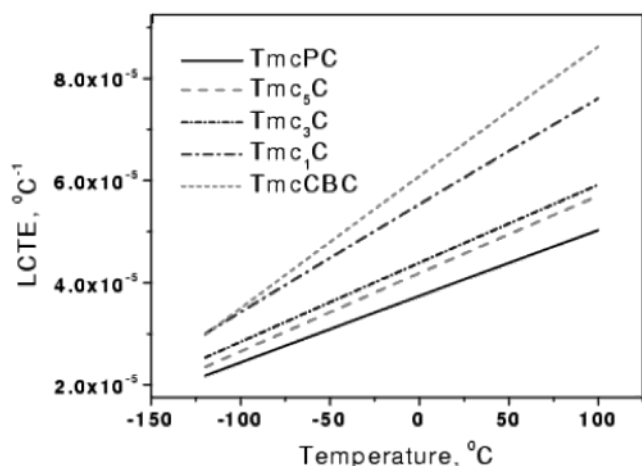


Figure 6. LCTE change with temperature for polymers of Tmc series.

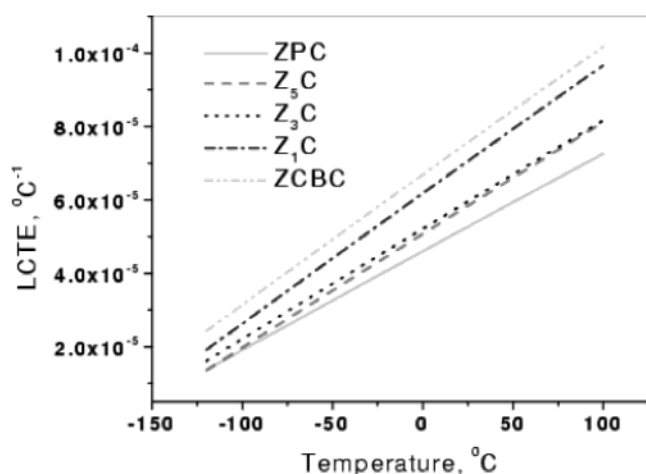


Figure 7. LCTE change with temperature for polymers of BPAZ series.

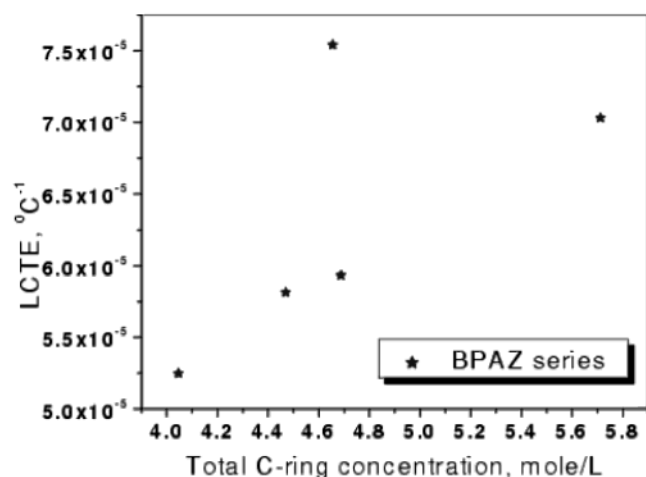


Figure 8. LCTE change with total C-ring concentration at room temperature for BPAZ polymers.

LCTE, but its total C-ring concentration is not the greatest. This may hint at a major contribution from BPA units on the thermal expansion. In the following discussion it will be shown that this does not appear to be the case. As seen in Figure 9, there is a good linear correlation between LCTE and main-chain C-ring concentration for both the Tmc and BPAZ polymers. Upon the replacement of half of the Tmc monomers by BPA

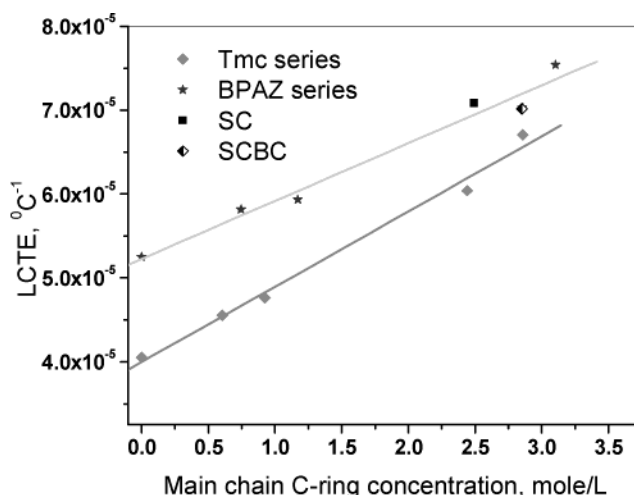


Figure 9. LCTE change with main-chain C-ring concentration at room temperature for SBI, Tmc, and BPAZ polymers.

monomers in Tmc₁C, TmcCBC is obtained, but TmcCBC is not caused to deviate from linearity to any significant degree by this replacement; this is also the case in ZCBC. Such observation makes it clear that the absence of correlation between LCTE and total C-ring content is not due to the replacement of BPAZ with BPA. LCTE is predominantly a manifestation of interchain interactions, as previously discussed.

The correlation in LCTE with the main-chain C-ring content instead of the total C-ring content indicates two things. First, main-chain C-ring incorporation decreases interchain forces; second, main-chain C-ring motion can modify the interchain interaction more effectively. The hypothesis that motions of in-chain segments can reduce the effective contact area and contact time between polymer chains, thus weakening their interchain interaction, can reasonably be made. The inversion of main-chain C-rings could introduce large-scale and rapid segmental motions, which should be more effective in modifying the interchain potentials. It appears that due to the chair–chair inversion of these main-chain C-rings, the local motional mode indeed may be altered, and to some extent, cooperative motions with their neighbors may be involved. However, side-chain C-ring motion would be expected to be less effective in promoting such an effect on its main-chain neighbors since only one end of the ring is anchored to the polymer chain. Figure 10 can help visualize the effect of main-chain C-ring inversion on its neighbors. In this figure, a trans-C-ring is linked to two bulky and rigid SBI entities. When the C-ring undergoes inversion from the top chair to the bottom chair through a twisted boat in the middle, there is a large spatial reorientation of its neighbors. This picture may be too simplistic. In reality, this reorientation may be much smaller in scale if the neighbors are too bulky and otherwise constrained; on the other hand, a relatively large scale of motion is not impossible given the right conditions, e.g., high temperature and poor initial packing. In Figure 9, one may note that even though the change in LCTE is mainly a result of the main-chain C-ring incorporation, the absolute values of LCTE are higher for the BPAZ series than those of the Tmc series. This may indicate different contributions from other units. The Tmc moiety is less mobile than the BPAZ moiety as reported previously.⁶ In Tmc, the side-chain C-ring is locked into a chair form, while the axial phenyl ring is able to undergo restricted

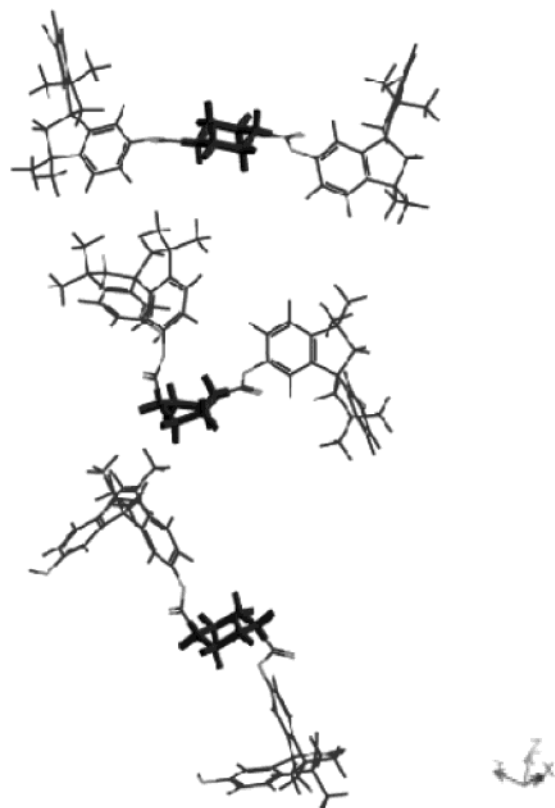


Figure 10. Illustration of chair-boat-chair conformational transition of a main-chain C-ring; bulky and rigid SBI entities are linked as neighbors.

rotation; however, in BPAZ, the side-chain C-ring undergoes rapid ring inversion, and the phenyl ring rotation is more free. So motions in the BPAZ entity can be activated more easily than those of Tmc units at the same temperature; therefore, motions from BPAZ weaken interchain forces more effectively than those in Tmc. The LCTE values of both SC and SCBC fall close to the line of the BPAZ series and are higher than the corresponding Tmc counterparts, even though the SBI moiety is bulkier than either BPAZ or Tmc. Also, within the whole temperature range studied, the LCTE values for SC and SCBC are almost exactly the same, while that for SC is even slightly greater than that for SCBC. The fact that the bulk CTE values may sometimes give different relationships will be shown in the next section; the real (as opposed to the apparent) relative order of CTE values of these polymers will be laid bare in discussing the thermal expansion of nanosized holes probed by PALS.

3.2. Coefficient of Thermal Expansion of Nanosized Holes. In the expression for bulk CTE, $\alpha = dV/VdT$, dV , the volume change, is predominantly due to the expansion of interchain space, while V is comprised of both the interchain space due to poor packing or steric hindrance and van der Waals volume. The latter describes the volume occupied by a molecule, which is impenetrable to other molecules with normal thermal energies. Thus, bulk CTE is reduced to roughly 1 order of magnitude smaller than those for holes. The CTE of open holes is a direct measure of chain mobility through which the effect of main-chain C-ring incorporation on chain dynamics will be seen more clearly.

A typical change in τ_3 with temperature is shown in Figure 12 for Tmc₅C. τ_3 increases with temperature from

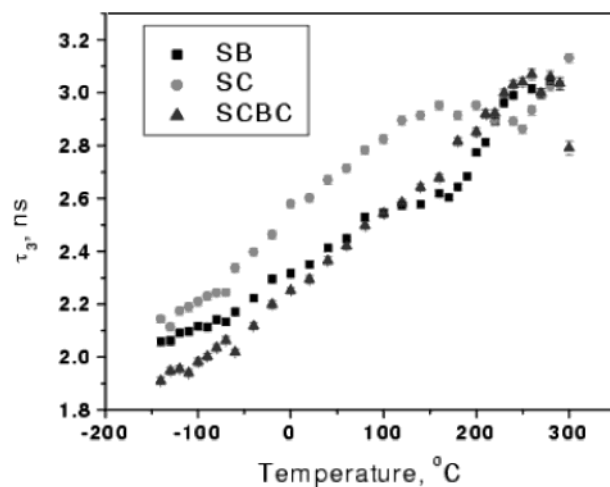


Figure 11. Change in the lifetime of o-Ps (τ_3) with temperature for SBI polymers.

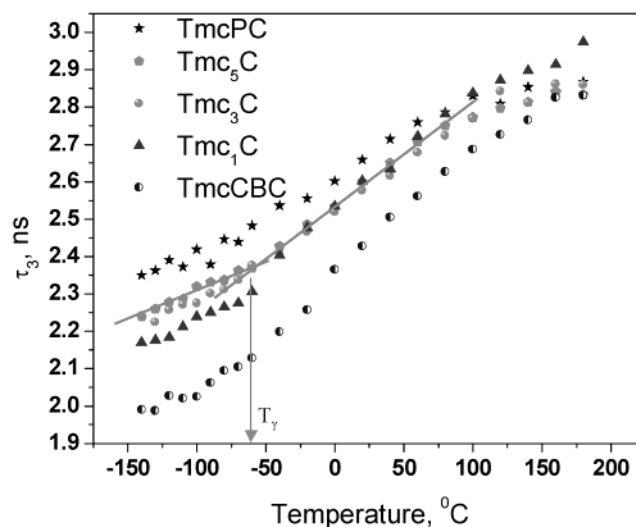


Figure 12. Change in the lifetime of o-Ps (τ_3) with temperature for Tmc polymers.

−140 up to 100 °C. Above 100 °C, the increase in τ_3 with temperature slows down, which may be related to some positron chemistry due to slight thermal degradation, as evidenced by some discoloration after the experiment. The exact reason is beyond the scope of this work; thus, no attempt will be made to discuss the results above this temperature. In most cases, the γ relaxation involving C-ring inversion can be detected as the one shown in Figure 12. The rate of the change in τ_3 with temperature increases abruptly around the γ relaxation temperature, T_γ . In Figures 11–13 are shown the changes in the lifetime of o-Ps with temperature for polymers of the SBI series, the Tmc series, and the BPAZ series. The literature data for TmcPC and ZPC from the work of Kluin et al.²⁶ compare very well with the present results. τ_3 values are systematically greater than those reported by Kluin et al. by around 0.1 ns. This difference could be due to the source contribution in our case, which was corrected in the work of Kluin et al.²⁶ It is also possible that differences in instrument setting created a systematic effect. If a constant CTE for nanosized holes is assumed in the glassy state, a value of 0.0015 K^{−1} is obtained for TmcPC in the present case, and a very similar value of 0.0017 K^{−1} is reported in the work of Kluin et al.

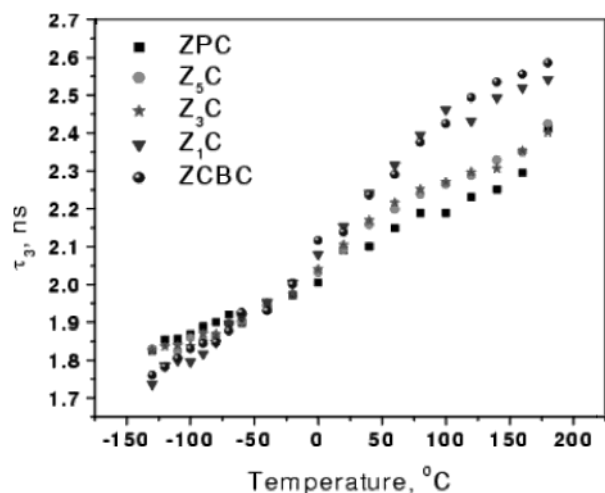


Figure 13. Change in the lifetime of o-Ps (τ_3) with temperature for BPAAZ polymers.

A common feature of all these polymers is that before the secondary relaxation takes place, the average hole sizes decrease with the increase in main-chain C-ring content. This feature is especially pronounced on the lower temperature side, but after the γ relaxation takes place, the rate of hole size expansion increases with the increase in main-chain C-ring content, which reverses at least partially the trend of the hole sizes on the lower temperature side.

At a very low temperature, especially when it approaches 0 K, the interchain space resulting from inefficient chain packing contributes most significantly to the total hole size. Therefore, the relative order of hole sizes is an indication of the packing efficiency of different polymers. As temperature increases, especially after the γ relaxation, the contribution toward the total hole size from the dynamic interchain expansion becomes larger and larger, and after a certain point, even the relative order of hole sizes may be changed. Chain packing efficiency is mainly determined by two factors, namely, chain topology and chain dynamics. An extended polymer chain is conducive to efficient chain packing, while chain dynamics provides the mobility necessary for improving the packing during the formation of the glass. The best arrangement for efficient packing is gradually approached with time as a consequence of such chain dynamics. As will be discussed in the next section, main-chain trans-C-rings do extend polymer chains, which should be beneficial to efficient chain packing. The extra mobility provided by the main-chain C-ring inversion will help polymer chains to assume the favorable energy state when they change from the melt state toward the glassy state. The thermal parameter that quantifies one effect of chain dynamics is the coefficient of thermal expansion of nanosized holes. Since the change in hole size with temperature is not as smooth as in the case of bulk dimensional change, a second-order polynomial cannot give a reasonable fit. In this part, no attempt will be made to calculate the CTE of open holes at all the temperatures; instead, only the values at 25 °C, a temperature at which all the mechanical tests were performed, will be calculated from the data. Shown in Figure 14 are the hole CTE of all the polymers. The bulk coefficients of thermal expansion of SC and SCBC are almost exactly the same within the temperature range of -120 to 100 °C, but the nanosized hole CTE of SCBC is apparently

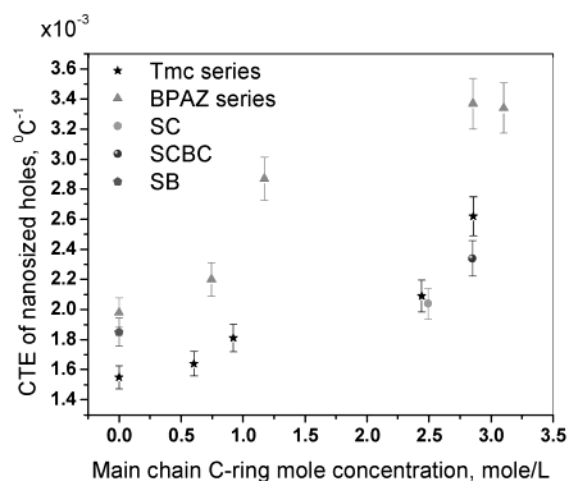


Figure 14. CTE of nanosized holes of all the polymers at 25 °C.

greater than that of SC at room temperature; in fact, it is the largest among SC, SB, and SCBC. As mentioned previously, the value of bulk CTE is reduced by the van der Waals volume, which contributes negligibly to the volume expansion. So the hole CTE is a better indication of the chain dynamics. The interchain distance estimated from the hole size is much larger for SC than for SCBC. This factor should reduce the interchain force even more in SC. But the overall interchain force is smaller for SCBC, judging from its greater hole CTE value. This, it can be surmised, is due to the enhanced intrachain dynamics in SCBC. In SCBC, there is a possible cooperative segmental motion in the CBC segment,³ which could significantly affect the interchain interaction by reducing the contact area and contact time, thus reducing the interchain force. The scale of this kind of segmental motion is much curtailed in SC since the segmental motion may be stopped at each SBI site due to its bulkiness. This point will become clearer in discussing the mechanical behavior.³⁶ As shown in Figure 14, with the increase in main-chain C-ring content, the CTE of nanosized holes in Tmc polymers and BPAZ polymers increases accordingly. The absolute values for BPAZ polymers are greater than those for the Tmc counterparts. This is due to the same reason as discussed in the bulk CTE case. The absolute values for SC and SCBC fall in the family of Tmc polymers, which is different from what has been observed in bulk CTE results, in which SC and SCBC fall in the family of BPAZ polymers instead. The relative order of the CTE values should be made according to hole CTE values instead of bulk CTE ones, since the former are better indicators of the chain dynamics. In this sense, polymers made from SBI are more akin to their Tmc counterparts. SBI and Tmc have the same molecular weights, and their structures are both rigid and bulky. Their polymers have similar T_g s; in fact, SCBC and TmcCBC even have similar mechanical properties.³⁶ Thus, CTE values of nanosized holes reveal the true nature of the relationship which is obscured by bulk CTE values.

3.3. Glass Transition Temperatures. In the foregoing, it has been shown that the secondary relaxation strength increases with the molar concentration of the total C-ring content,⁶ while thermal expansion coefficient increases with the increase in the amount of main chain C-rings. Given these observations, a legitimate question to ask is: how does the glass transition temperature change with the main-chain C-ring con-

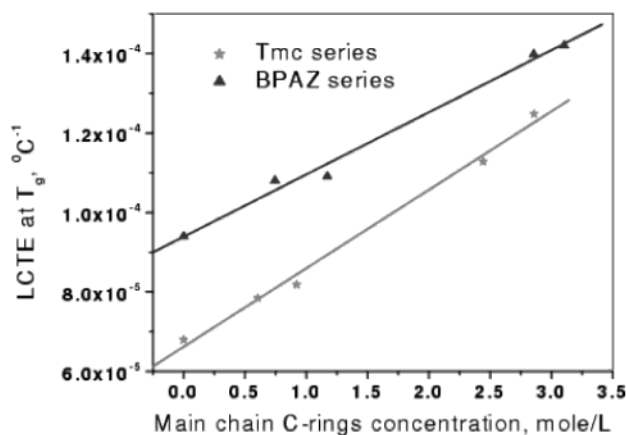


Figure 15. LCTE at glass transition temperature vs main C-ring mole concentration.

tent? Simha and Boyer³⁷ have proposed eq 2 by assuming that the so-called free volume fraction at T_g is a universal constant:

$$T_g \Delta \alpha = 0.113 \quad (2)$$

where $\Delta \alpha$ is the difference between the thermal expansion coefficients at T_g for the melt and glass. They also proposed that

$$\alpha_1 T_g = 0.164 \quad (3)$$

where α_1 is the CTE of the melt at T_g . Therefore

$$(\alpha_1 - \alpha_g) T_g = 0.113 \quad (4)$$

$$\alpha_g T_g = 0.164 - 0.113 = 0.051 \quad (5)$$

This means that if α_g increases, T_g will decrease.

Because some of the polymers have T_g as high as 280 °C, getting CTE at this high temperature is difficult due to the thermal degradation of these polymers. However, the LCTE at the glass transition temperature can still be estimated by extrapolating from the results at lower temperatures. As shown in Figures 6 and 7, LCTE increases linearly with temperature within the range of -120 to 100 °C. Assuming that this trend persists into the glass transition region should not introduce significant errors.³⁸ Shown in Figure 15 is the plot of LCTE at T_g versus the main-chain C-ring mole concentration for polymers of the Tmc and the BPAZ series. Clearly, it can be seen that the trend observed at room temperature is maintained up to the glass transition temperatures. With the increase in main chain C-ring content, LCTE at T_g also increases. A consequence of this observation and eq 5 is that the T_g s will decrease with the increase in main-chain C-ring concentration. This would imply that the enhancement of the main-chain motion is accompanied by the lowering of the softening temperature. However, as shown in Figure 16, in both the Tmc and the BPAZ series, the glass transition temperatures increase as more main-chain C-rings are incorporated. TmcCBC and ZCBC do not follow this trend because the incorporation of the BPA moiety decreases the T_g s. Figure 17 is the plot of $\alpha_g T_g$ vs main-chain C-ring concentration. For TmcPC and ZPC, $\alpha_g T_g$ has values of 0.05, consistent with Simha–Boyer's rule. But with the increase in the main-chain C-ring incorporation, $\alpha_g T_g$ increased. Tmc and BPAZ polymers behave identically. This observation is inconsistent with

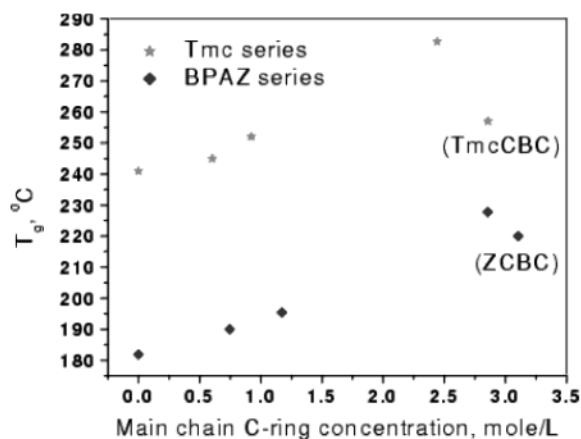


Figure 16. Glass transition temperature change with main-chain C-ring incorporation.

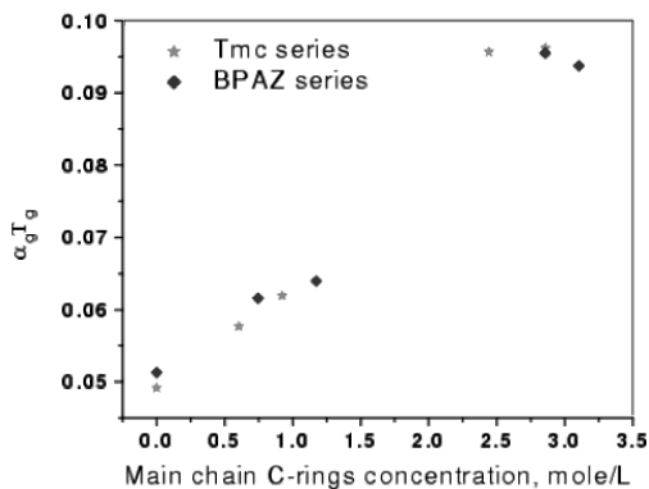


Figure 17. $\alpha_g T_g$ vs main-chain C-ring concentration for Tmc and BPAZ polymers.

Simha–Boyer's rule. As discussed in the Introduction, various correlations between T_g and molecular parameters fail to work for polymers with main-chain aromatic groups. This failure may be because the parameters C_∞ and σ cannot describe chain stiffness correctly for these polymers. On the other hand, the persistence length L_p or the Kuhn length may be a better and natural measures of chain stiffness.

The calculation of L_p is not a trivial task. It demands a detailed knowledge of polymer chain energetics. However, the increase in T_g with L_p has been shown experimentally.^{39,40} In another case, partial substitution of the carbonate units in polycarbonate by terephthalate groups leads to a systematic increase in T_g ; qualitatively, this has been ascribed to the increase in persistence length.^{41,42} Upon replacement of up to 50% of the carbonate groups in BPA-PC by terephthalate groups, the T_g was increased from 150 to 192 °C. From Figure 18, it can be seen qualitatively that the replacement of carbonate groups by terephthalate groups can lead to increased persistence length. In BPA-PC, the carbonate groups can take either a trans or cis conformation. The cis conformation introduces a kink into the polymer chain, thus reducing the persistence length. The incorporation of terephthalate groups can extend the straight segment between the kinks by at least the length of this rigid group, thus increasing L_p . A trans-C-ring has a close resemblance in shape to that of a phenyl ring. Thus, the incorporation of trans C-rings should have the

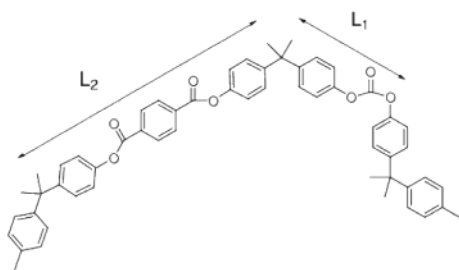


Figure 18. Part of a poly(ester carbonate) chain: notice the change in stiff segment length introduced by terephthalate group.⁴¹

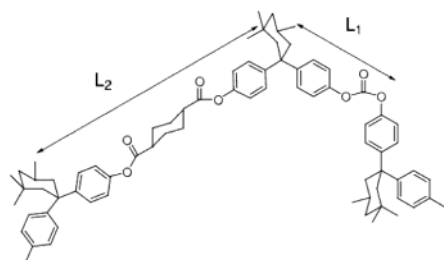


Figure 19. Part of a poly(ester carbonate) chain of Tmc: notice the increased stiff segment length introduced by trans-main-chain C-rings.

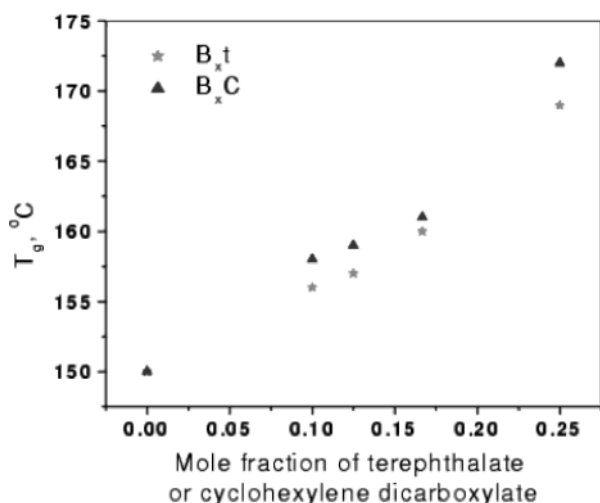
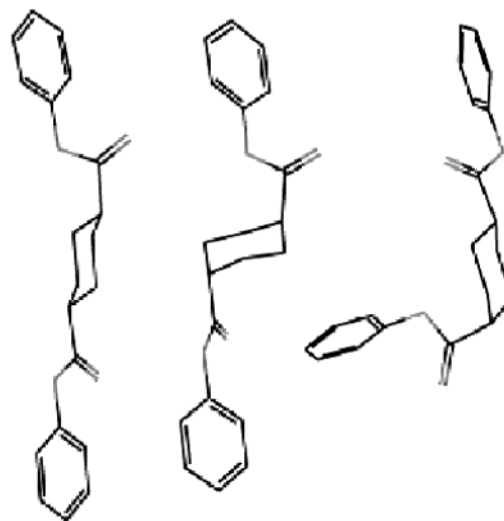


Figure 20. T_g 's of B_xt and B_xC; x is the block length of polycarbonate.^{43,44}

same function as that of phenyl groups in extending polymer chains. This can be seen clearly in Figure 19 for Tmc polymers. The results of Wu⁴³ and Liu⁴⁴ further substantiate the hypothesis posed here. In their B_xt polymers, terephthalate groups were periodically inserted into the polycarbonate of BPA, where x is the number of repeating units in each polycarbonate block. In B_xC, instead of terephthalate groups, cyclohexylene dicarboxylate groups were inserted into BPA-PC. From Figure 20, it can be seen that the two series of polymers have almost identical T_g s at the same mole fraction of terephthalate groups or main-chain C-ring groups. Thus, a main-chain trans-C-ring, just like a phenyl ring, extends the polymer chain and produces increased persistence length and therefore the increased T_g . Now a crucial question needs to be answered: why do the polymers studied in this work behave so differently than typical polymers in that both the glass transition temperature and thermal expansion coefficient increase at the same time? It has been discussed in the thermal



trans-equatorial equatorial trans-axial axial cis-equatorial axial

Figure 21. Different configurations and conformations and their effect on the length of stiff segment.⁴⁸

Table 2. Molecular Weight and Glass Transition Temperature of Polymers Based on SBI with Pure Trans-C-Rings and C-Rings with Cis:Trans = 72:28; m Stands for Mixture of C-Rings

polymer	M_n	M_w	$T_g/^\circ\text{C}$
SC	51K	778K	275
SC-m	35K	49K	227
SCBC	39K	77K	246
SCBC-m	31K	76K	198
SC(BC) ₂	32K	63K	224
SC(BC) ₂ -m	33K	83K	186

expansion section that main-chain C-ring incorporation weakens intermolecular forces. Therefore, the incorporation of main-chain C-rings will work against enhancing T_g from the cohesive energy density point of view. This leads to the conclusion that the increase in T_g with increase in the main-chain C-ring content is mainly due to the stiffening of polymer chains by these C-rings.

The main-chain C-ring undergoes rapid inversion even at room temperature; at T_g , these inversions are even faster. After an inversion, a trans-C-ring with two equatorial substituents becomes a trans-C-ring with two axial substituents, introducing a step instead of a kink into the polymer chain. As shown in Figure 21, this step only slightly reduces the chain stiff segment length. Furthermore, the conformational free energy for an ester group is around 1.1–1.2 kcal/mol.⁴⁵ There are two ester groups on a main-chain C-ring, so the equatorial–equatorial trans-C-ring is favored in energy by about 2.2–2.4 kcal/mol, which indicates that at least 90% of the trans-C-rings are in the equatorial–equatorial conformation. So the trans-C-ring plays the role of stiffening polymer chains. By contrast, a cis-C-ring has one substituent at the equatorial position and another at the axial position. Thus, the cis-C-ring introduces a kink into the polymer chain, significantly reducing the length of the stiff segment. It can therefore be expected that a great deal of decrease in glass transition according to the present argument would occur. This is indeed the case by looking at Table 2. Polymers based on SBI with the same chemical structure but with different C-ring configurations show drastically different T_g s. Polymers with C-rings of cis:trans = 72:28 have glass

transition temperatures at least 40 °C lower than their trans counterparts.

4. Summary

The coefficients of thermal expansion correlate well with the main-chain C-ring mole concentration but not the total C-ring concentration, in contrast to the secondary relaxation strength. The increased thermal activity has been ascribed to the increased segmental molecular motion introduced by main-chain C-ring inversion. The glass transition temperature is mainly influenced by the chain stiffness in the polymers studied in this work. Main-chain trans-C-rings extend the polymer chain by increasing the length of the stiff segments. The extended shape of the polymer chains also results in better chain packing as indicated by nanoscale hole size at low temperatures. The multifaceted ability of trans-main-chain C-ring to increase molecular motion, glass transition temperature, and chain packing is proposed to be due to its unique shape and its ability to undergo ring inversion. The unique shape provides the function of extending the polymer chains, while the ring inversion introduces enhanced local chain motion, which reduces the interchain interactions by decreasing the contact surface area and contact time between polymer chains.

Acknowledgment. We acknowledge the technical help of Dr. Terry Dull in the PALS experiments and the financial support from the U.S. Air Force Office of Scientific Research (AFOSR) (Grant F49620-98-1-0158) for this research.

References and Notes

- (1) Xiao, C. D.; Jho, J. Y.; Yee, A. F. *Macromolecules* **1994**, *27*, 2761.
- (2) Chen, L. P.; Yee, A. F.; Moskala, E. J. *Macromolecules* **1999**, *18*, 5944.
- (3) Liu, J. W.; Yee, A. F. *Macromolecules* **1998**, *31*, 7865.
- (4) Liu, J. W.; Yee, A. F. *Macromolecules* **2000**, *33*, 1338.
- (5) Chen, L. P.; Yee, A. F.; Goetz, J. M.; Schaefer, J. *Macromolecules* **1998**, *31*, 5371.
- (6) Li, X. Y.; Yee, A. F. *Macromolecules* **2003**, *36*, 9411.
- (7) Swan, P. R. *J. Polym. Sci.* **1962**, *56*, 403.
- (8) Warfield, R. W. *Makromol. Chem.* **1974**, *175*, 3285.
- (9) Wada, Y.; Itani, A.; Nishi, T.; Nagai, S. *J. Polym. Sci., Part A-2* **1969**, *7*, 201.
- (10) Barker, R. E., Jr. *J. Appl. Phys.* **1967**, *38*, 4234.
- (11) Stachurski, Z. H. *Prog. Polym. Sci.* **1997**, *22*, 407.
- (12) Ashby, M. F. *Materials Selection in Mechanical Design*, 2nd ed.; Butterworth-Heinemann: Woburn, MA, 1999.
- (13) Privalko, V. P.; Lipatov, S. *J. Macromol. Sci., Phys. B* **1974**, *9*, 551.
- (14) Boyer, R. F. *Macromolecules* **1992**, *25*, 5326.
- (15) Lu, X.; Jiang, B. Z. *Polymer* **1991**, *32*, 471.
- (16) Chee, K. K. *J. Appl. Polym. Sci.* **1991**, *43*, 1205.
- (17) Birshtein, T. M. *Vysokomol. Soyed. A* **1977**, *19*, 54.
- (18) Kratky, O.; Porod, G. *Recl. Trav. Chim.* **1949**, *68*, 1106.
- (19) Flory, P. J. *Statistical Mechanics of Chain Molecules*; Hanser Publishers: Munich, 1989.
- (20) Xu, Z. D.; Hadjichristidis, N.; Fetters, L. J.; Mays, J. W. *Adv. Polym. Sci.* **1995**, *120*, 1.
- (21) Kluin, J. E.; Yu, Z.; Vleeshouwers, S.; McGervey, J. D.; Jamieson, A. M.; Simha, R. *Macromolecules* **1992**, *25*, 5089.
- (22) Wang, Y. Y.; Nakanishi, H.; Jean, Y. C. *J. Polym. Sci., Part B: Polym. Phys.* **1990**, *28*, 1431.
- (23) Xie, L.; Gidley, D. W.; Hristov, H. A.; Yee, A. F. *J. Polym. Sci., Part B: Polym. Phys.* **33**, 95, 77.
- (24) Tao, S. J. *J. Chem. Phys.* **1972**, *56*, 5499.
- (25) Eldrup, M.; Lightbody, D.; Sherwood, J. N. *Chem. Phys.* **1981**, *63*, 51.
- (26) Kluin, J. E.; Yu, Z.; Vleeshouwers, S.; McGervey, J. D.; Jamieson, A. M.; Simha, R.; Sommer, K. *Macromolecules* **1993**, *26*, 1853.
- (27) Yu, Z.; Yahsi, U.; McGervey, J. D.; Jamieson, A. M.; Simha, R. *J. Polym. Sci., Part B: Polym. Phys.* **1994**, *32*, 2637.
- (28) Ujihira, Y.; Ryuo, T.; Kobayashi, Y.; Nomizu, T. *Appl. Phys.* **1978**, *16*, 71.
- (29) Xie, L. Measurements of Microscopic Voids in Polymers Using Positron Annihilation Lifetime Spectroscopy. Ph.D., The University of Michigan, Ann Arbor, MI, 1995.
- (30) Kindl, P.; Reiter, G. *Phys. Status Solidi A* **1987**, *104*, 707.
- (31) Welander, M.; Maurer, F. H. J. *Mater. Sci. Forum* **1992**, *105–110*, 1811.
- (32) Kobayashi, Y.; Wang, C. L.; Hirata, K. M.; Zheng, W.; Zhang, C. *Phys. Rev. B: Condens. Matter Mater. Phys.* **1998**, *58*, 5384.
- (33) Maurer, F. H. J.; Schmidt, M. *Radiat. Phys. Chem.* **2000**, *58*, 509.
- (34) Puff, W. *Comput. Phys. Commun.* **1983**, *30*, 359.
- (35) Liu, L. B.; Gidley, D. W.; Yee, A. F. *J. Polym. Sci., Part B: Polym. Phys.* **1992**, *30*, 231.
- (36) Li, X. Y.; Yee, A. F. Manuscript in preparation.
- (37) Simha, R.; Boyer, R. F. *J. Chem. Phys.* **1962**, *37*, 1003.
- (38) Coquil, S. L.; Adams, D. F. Mechanical properties of several neat polymer matrix materials and unidirectional carbon fiber-reinforced composites. NASA Contractor Report 181805, 1989.
- (39) Kakali, F.; Kallitsis, J. K. *Macromolecules* **1996**, *29*, 4759.
- (40) Kakali, F.; Gravalos, K. C.; Kallitsis, J. K. *J. Polym. Sci., Part A: Polym. Chem.* **1996**, *34*, 1581.
- (41) Prevorsek, D. C.; De Bona, B. T. *J. Macromol. Sci., Phys. B* **1981**, *19*, 605.
- (42) Freitag, D.; Westeppe, U. *Makromol. Chem., Rapid Commun.* **1991**, *12*, 95.
- (43) Wu, J. Correlated Motions and Relaxation Behavior in Polycarbonate Copolymers. Ph.D. Thesis, The University of Michigan, Ann Arbor, MI, 1997.
- (44) Liu, J. W. The Effect of Enhanced Molecular Mobility on Mechanical Properties. Ph.D. Thesis, The University of Michigan, 1999.
- (45) Carey, F. A.; Sundberg, R. J. *Advanced Organic Chemistry*, 3rd ed.; Plenum: New York, 1993; Vol. 1.
- (46) Molecular Simulations Inc., 9685 Scranton Road, San Diego, CA 92121-3752.
- (47) Mayo, S. L.; Olafson, B. D.; Goddard, W. A. *J. Phys. Chem.* **1990**, *94*, 8897.
- (48) The conformations and configurations were generated and energetically minimized using Cerius² molecular modeling software (version 3.5) from Molecular Simulations Inc.⁴⁶ with the atom force potentials being described by the DREIDING II force field.⁴⁷

MA034557L